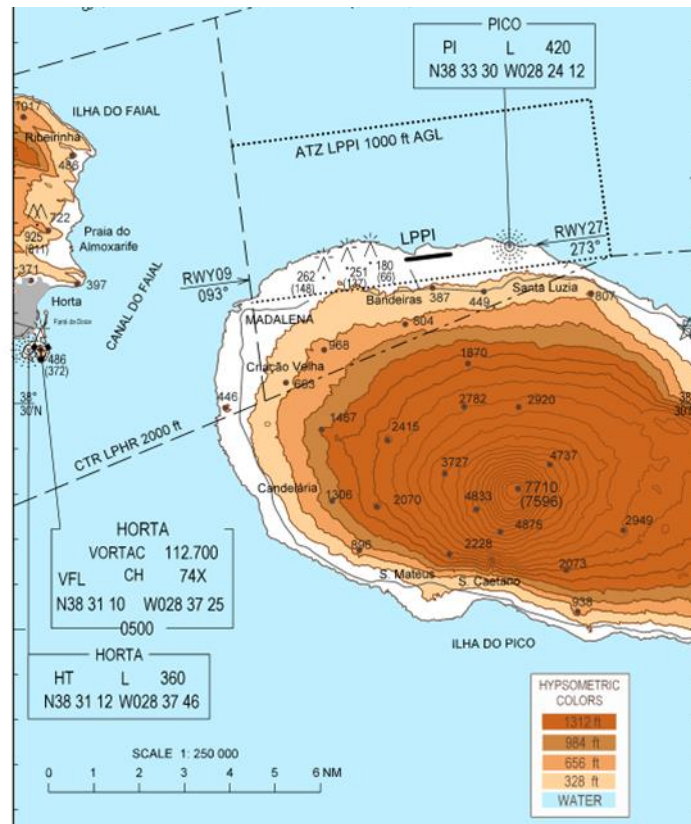
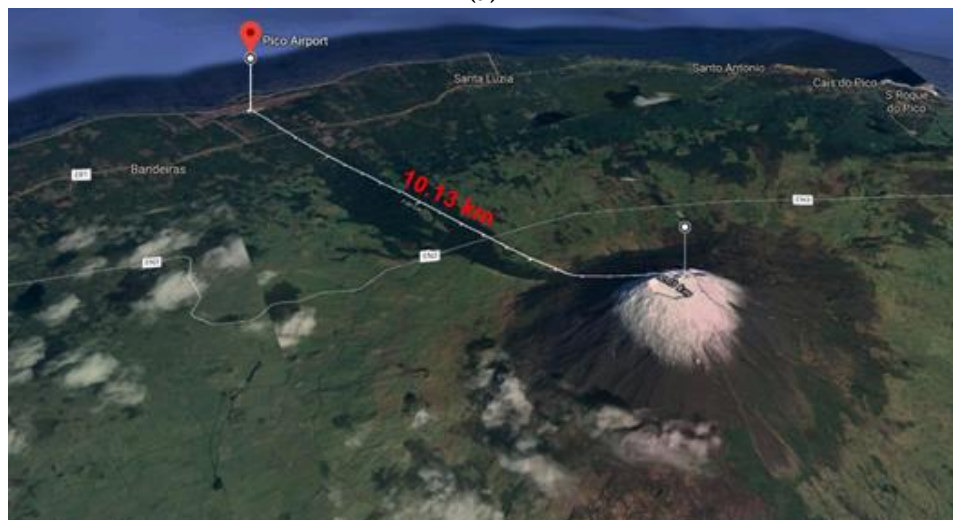


Supplementary Materials for “Analysis of Mountain Wave Effects on a Hard Landing Incident in Pico Aerodrome using the AROME Model and Airborne Observations”

14-06-2019



(a)



(b)

Figure S1. (a) Enlarged view of Pico Mountain and its Aerodrome (LPPI), from NAV Portugal (<https://www.nav.pt/docs/AIS/aerodromos/pico.pdf?sfvrsn=20>); (b) Location of Pico Aerodrome (LPPI) relative to Pico Mountain, from Google Earth.

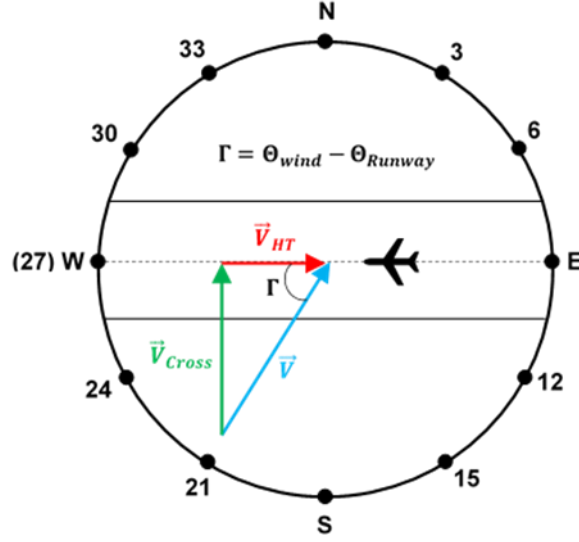


Figure S2: Cross and headwind components.

The calculation of the head or tailwind component V_{HT} that appears in Eq. 2 in the main article is done by resolving the wind vector \vec{V} according to the angle Γ (see Figure S2), which depends on the runway bearing Θ_{runway} and wind direction Θ_{wind} both in degrees. Expressions for V_{HT} and V_{Cross} (the crosswind component) are provided respectively by:

$$V_{HT} = -|\vec{V}| \cos \left[(\Theta_{wind} - \Theta_{Runway}) \cdot \frac{\pi}{180} \right], \quad (S2.1)$$

$$V_{Cross} = |\vec{V}| \sin \left[(\Theta_{wind} - \Theta_{Runway}) \cdot \frac{\pi}{180} \right]. \quad (S2.2)$$

The runway bearing in degrees is determined in relation to the runway code according to Eq S2. 3. For Pico Aerodrome, this can be either 27 or 9.

$$\Theta_{Runway} = Runway\ Code \times 10 \quad (S2.3)$$

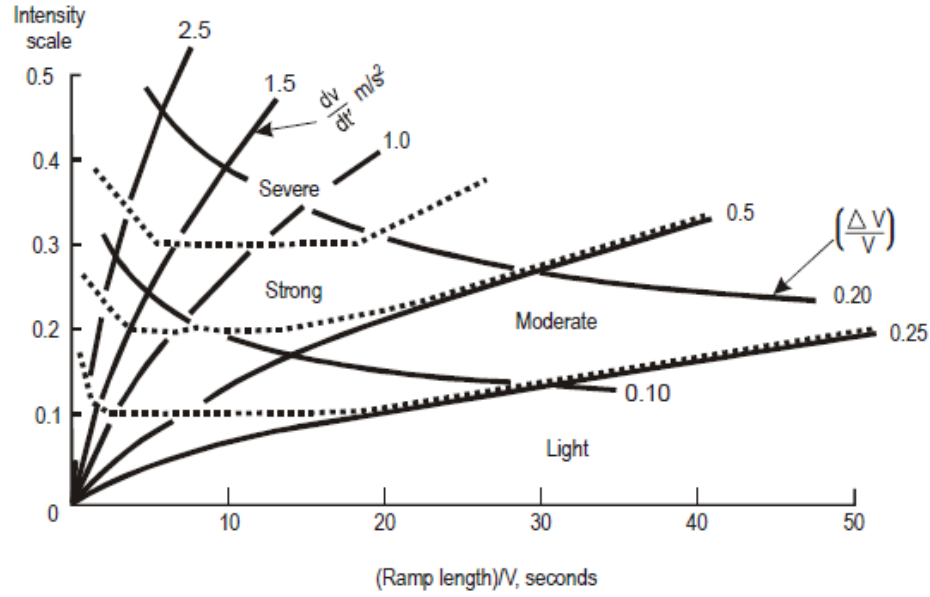


Figure S3. Boundaries for the classification of wind shear intensity as recommended by the ICAO Manual on Low-level Wind Shear [24] and originally proposed by Woodfield and Woods [23] (see main article for references).

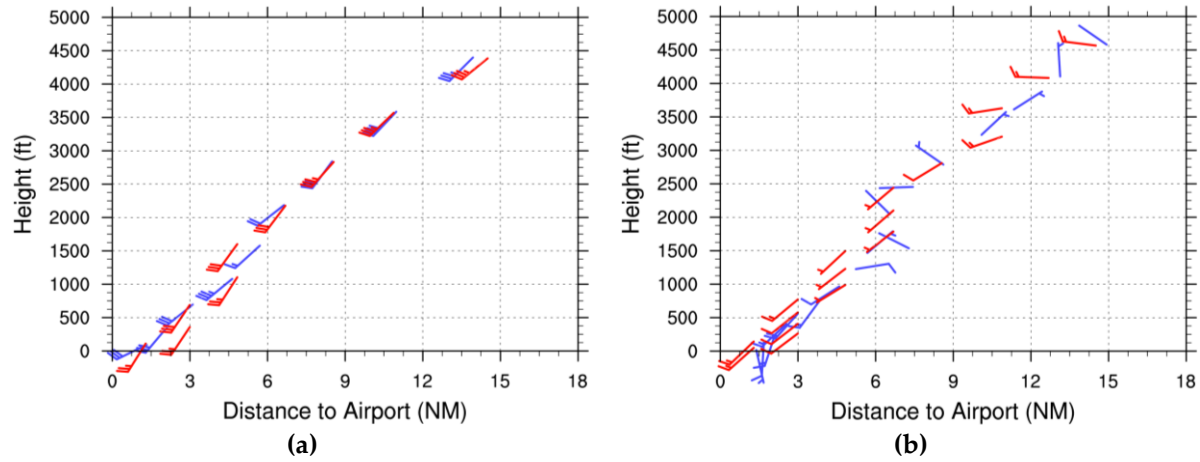


Figure S4. Wind profile along flight path (see Figure 2) according to aerial observations and AROME for: (a) Flight 1; (b) Flight 2. Wind barbs in blue depict aerial observations while those in red represent AROME forecasts.

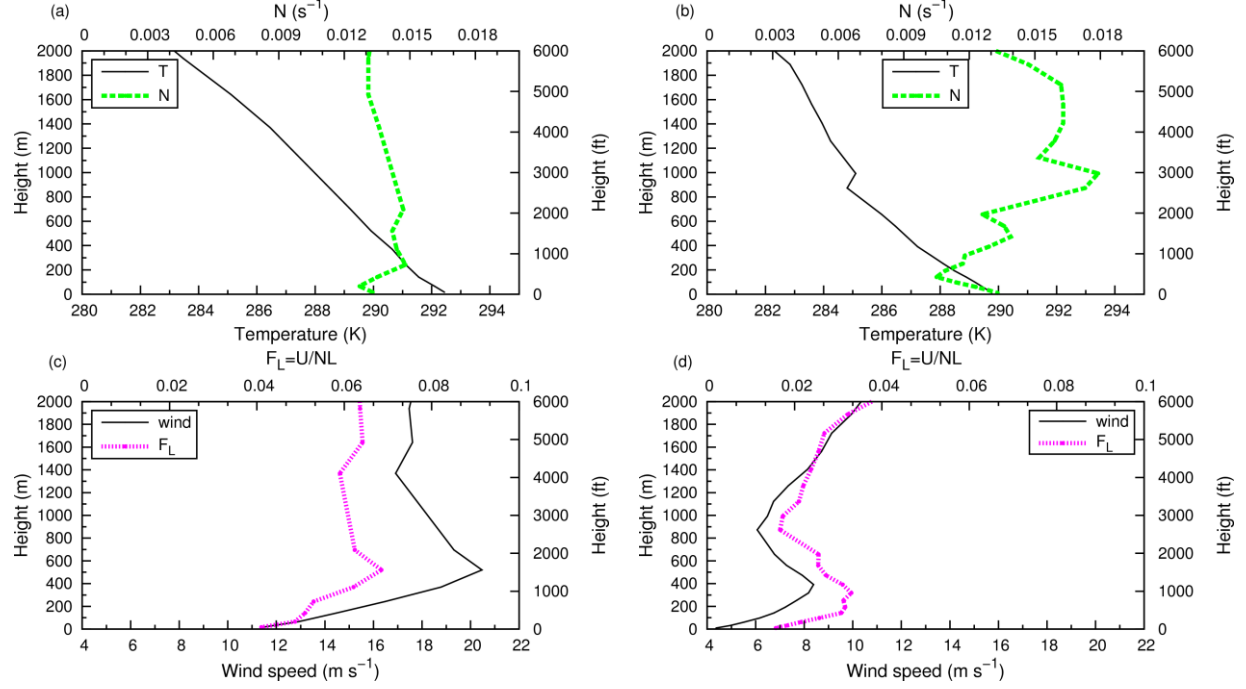


Figure S5. Absolute temperature and N profiles at point C for: (a) Flight 1; (b) Flight 2. Wind speed and F_L profiles at point C for: (c) Flight 1; (d) Flight 2.

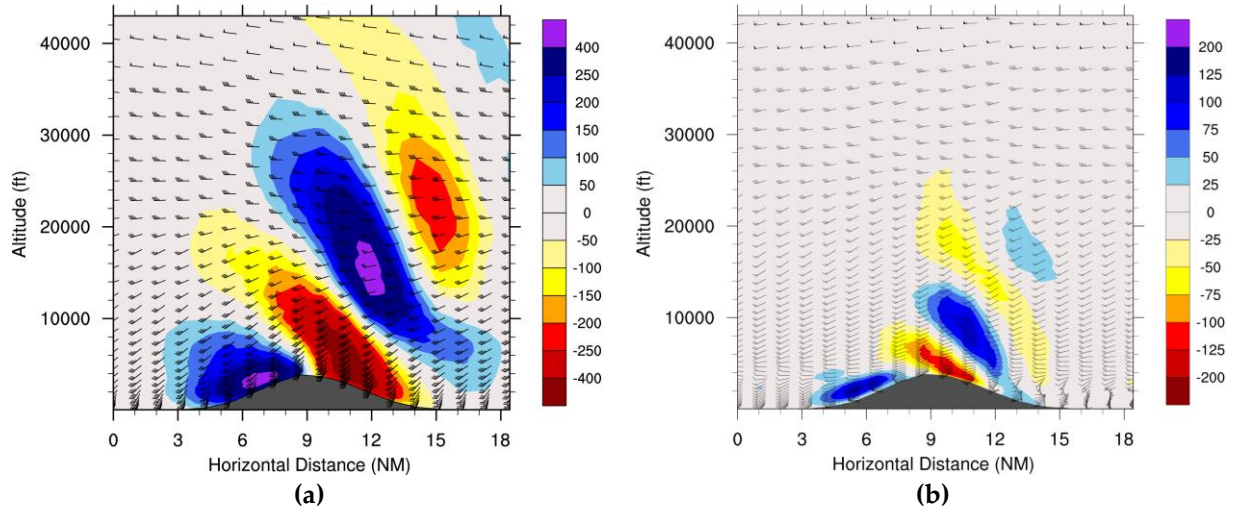


Figure S6. (a) Vertically propagating mountain waves predicted by AROME model during Flight 1; (b) and during Flight 2. Shading denotes up or downdraft intensity with a positive sign corresponding to an updraft.

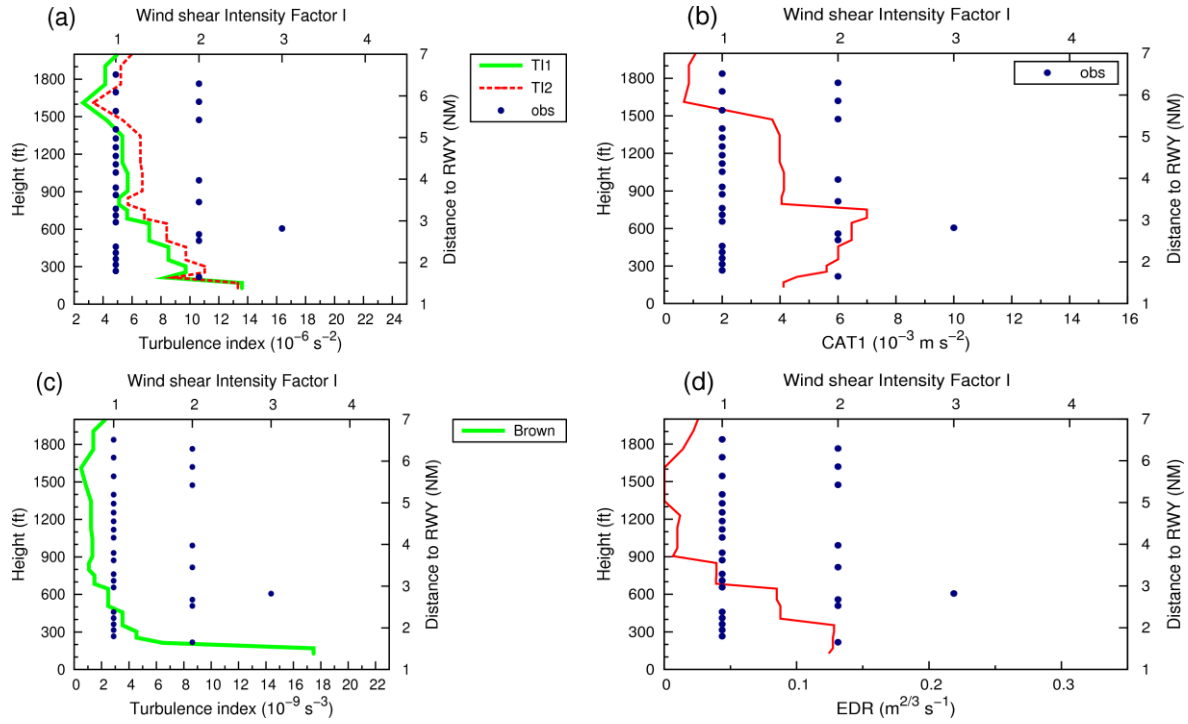


Figure S7. AROME turbulence indicators (bottom x-axis) versus the Wind shear Intensity Factor I (top x-axis), along the flight path during Flight 2. The green dots indicate the Wind Shear Intensity Factor “I”.

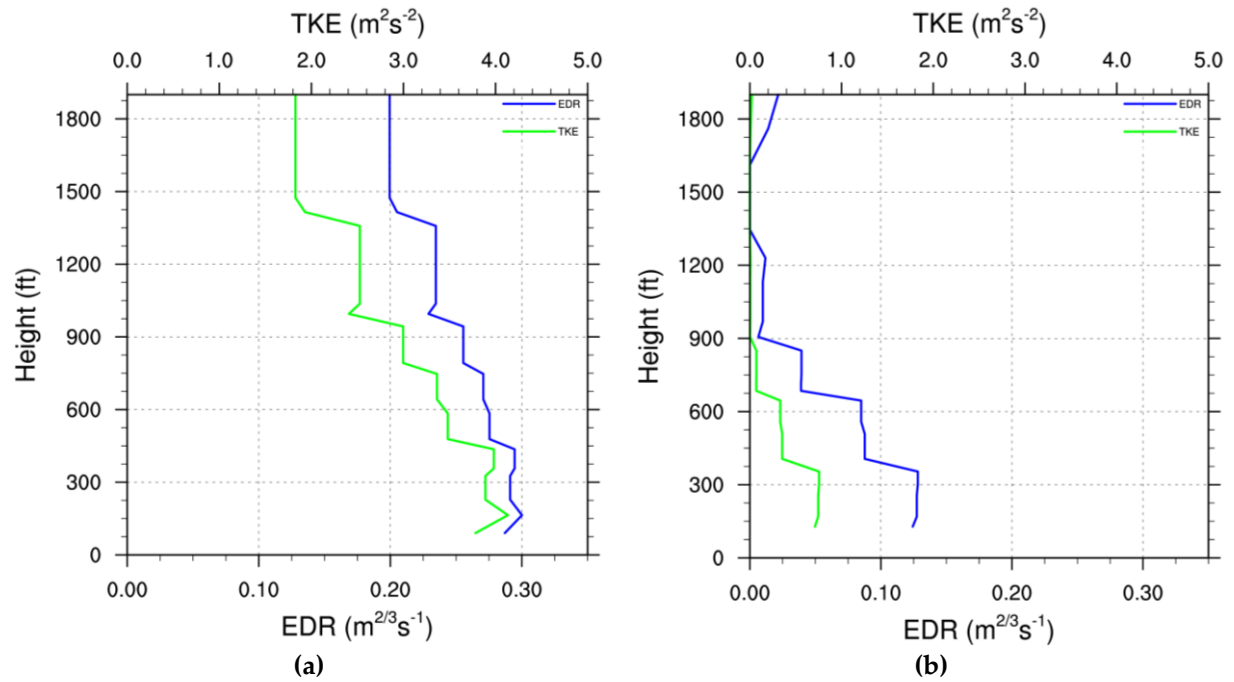


Figure S8: Variation of Turbulent Kinetic Energy (TKE) and Eddy Dissipation Rate (EDR) with height for (a): Flight 1 and (b) Flight 2.

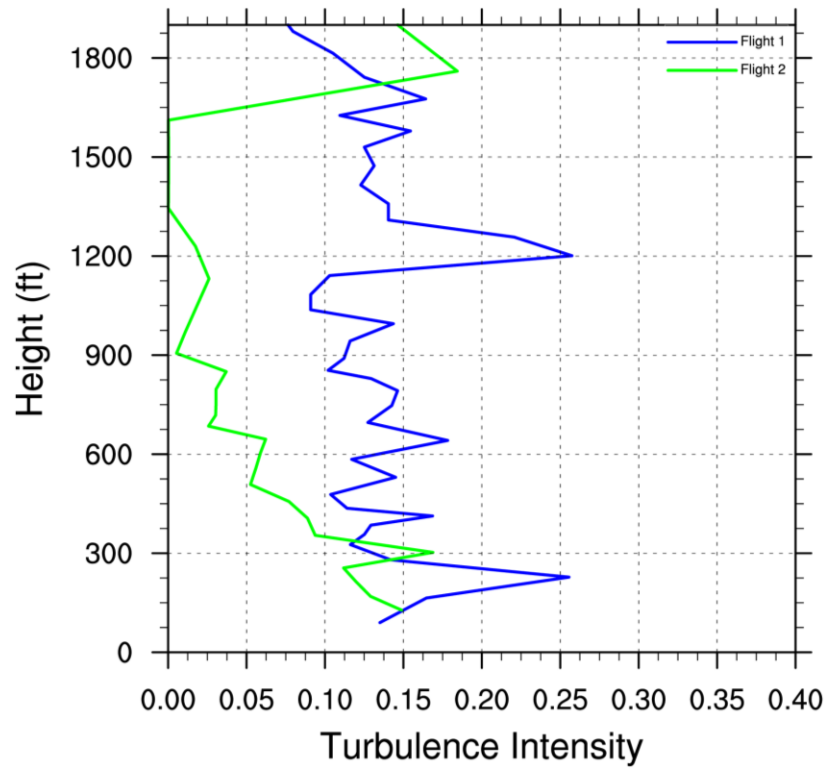


Figure S9: Turbulence Intensity for both Flights.

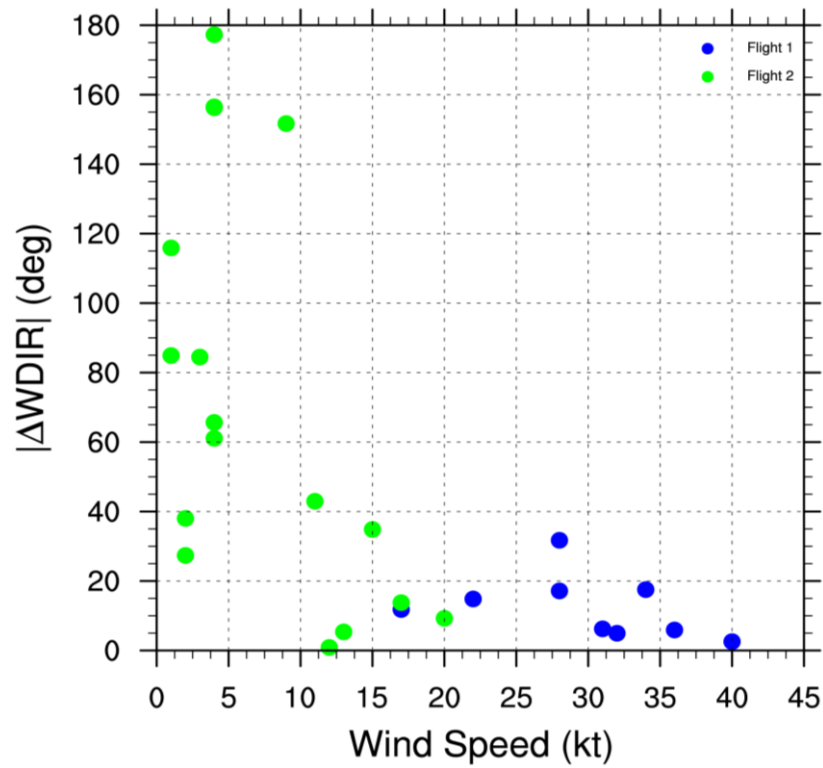


Figure S10: Absolute value wind direction errors versus wind speed for both Flights.